JOURNAL OF OPTOELECTRONICS AND ADVANCED MATERIALS Vol. 9, No. 6, June 2007, p. 1660 - 1664

A preliminary study of the structure and the corrosion performance of plasma sprayed YSZ coatings

G. VOURLIAS, N. PISTOFIDIS, D. CHALIAMBALIAS,
I. TSIAOUSSIS, G. STERGIOUDIS, E. K. POLYCHRONIADIS
Physics Department, Aristotle University of Thessaloniki, 54124 Thessaloniki, Greece

An important problem related with hot-dip galvanizing is the storage of liquid zinc, because steel is heavily corroded by the molten metal. To overcome this problem the ferrous containers are coated with ceramic materials. In the present work the structure and the corrosion performance of YSZ coatings on low carbon steel is examined. For that purpose coupons of steel St-37 were plasma sprayed with ZrO_2-8%Y_2O_3. The structural characterization prior to corrosion took place with Scanning Electron Microscopy, X-Ray Diffraction and Transmission Electron Microscopy. Afterwards the as-coated samples were dipped in molten zinc at 450^{o}C up to 120 hrs. The initial examination of the YSZ coatings showed that many pores are present in their mass, which, however, do not communicate with each other and as a result they do not facilitate zinc diffusion up to the substrate. Furthermore the coating is exclusively composed by YSZ with a little different stoichiometry ($ZrO_{1.88}$-8%Y_2O_3) from the theoretical. No diffusion in the substrate took place and consequently the coating is only mechanically bonded to the substrate. For the corrosion study kinetic curves representing molten Zn attack on coated and uncoated carbon steel were drawn. From this data it turned out that YSZ coating are almost unaffected.

(Received November 14, 2006; accepted April 26, 2007)

Keywords: Metals and alloys, Plasma spray, YSZ, Coating materials, X-ray diffraction, SEM, TEM

1. Introduction

A very important problem that is related with hot-dip galvanizing is the storage of liquid zinc. For this purpose kettles of low carbon and low silicon steel (such as Armco steel-C: 0.08%, Mn: 0.4%, P: 0.015%, S: 0.025%, Si: traces) are used [1]. The cross-section of these kettles is U-formed to avoid weldind. However, even with these precautions, steel is heavily corroded by the liquid phase, a usual phenomenon in industrial processes which involve handling of molten metals (molten metal corrosion [2]). As a result the kettles have to be replaced in average every 6 years [1]. Although ferrous materials are very prone in molten zinc corrosion, ceramics are rather inert under the same conditions. The construction however of ceramic kettles is very expensive, if we take into account the dimensions of the zinc kettles (10m x 3m x 2m in average [1]). Furthermore heating of the zinc is rather difficult [1], since ceramics are thermal barriers and heat transfer is impeded. As a result instead of constructing ceramic kettles, ceramic coatings are often used for the corrosion protection of iron and steel in contact with the molten metal [2, 3]. Yttria stabilized Zirconia (YSZ) has been found to be extremely resistant at high temperature and inert with regard to liquid metals. Thus YSZ coatings prolong material life cycle and reduce material cost in that kind of engineering applications [4-10]. However YSZ coatings find no application in the galvanizing industry, although their performance for the liquid metal corrosion protection of the zinc kettle is expected to be very good. For that purpose in the present work the attack of liquid zinc on YSZ coatings on low carbon steel is examined. Apart from the collection of kinetic data, in the present research an attempt is made to correlate the coating corrosion behavior with the coating structure. Hence a detailed study of the YSZ microstructure is also presented.

2. Experimental

Plates of steel St-37 (15 cm x 3 cm x 0.3 cm) were used as coating substrates and were prepared prior to YSZ deposition with grit blasting with Al_2O_3 particles in order to create an anchor tooth profile at the surface of the substrate. The coating was formed with the air plasma spraying technique. In this case, an electric arc of high intensity (a few hundred Amperes) between a tungsten cathode and a copper anode ionizes a gas mixture (plasma gas) which forms the plasma jet. The YSZ powder is fed right at the exit point of the jet from the aperture of the device where it melts. The droplets formed, after being accelerated by the plasma gas, strike the surface of the steel substrate, flatten and form thin lamellae that conform, adhere and interlock with each other and the substrate surface building up a ceramic layer up to a thickness of about 150–200 μm. The plasma gas used was an Ar mixture with H_2 (total gas flow 45 l/min). The current intensity for the plasma formation is 120-200 A and the power supply about 40 kW. The deposited material was commercially available grade YSZ (ZrO_2-8 mol% Y_2O_3) in the form of gas-atomized powder with an average diameter of -90+15 μm as it was determined microscopically and its feed rate was 20 g/min. The gun-substrate distance was 100–120 mm. After the coating

deposition, cross-sections of the as-sprayed specimens have been cut, mounted in bakelite and polished up to 5 μm alumina emulsion for morphological observation. Their characterization took place with scanning electron microscopy (SEM), X-ray diffraction (XRD), conventional transmission electron microscopy (CTEM) and high resolution electron microscopy (HREM). SEM observations were performed with a 20 kV JEOL 840A SEM equipped with an OXFORD ISIS 300 EDS analyzer and the necessary software. Stoichiometric microanalysis and chemical mapping was performed on the polished cross-sections of the coating. XRD took place with a Siemens D-8000 diffractometer using a Cu Kα radiation (λ=1.54186Å). The samples were examined three times. During the first examination the initial cross-section was examined. Afterwards part of the coating surface was abrasively removed and the samples were re-examined in order to exclude the effect of phases formed only at the coating surface and to detect any phase present only at the Fe/YSZ interface. Finally, selected specimens were examined with CTEM by using a 100 kV JEOL 100CX TEM and with HRTEM by using a 200 kV JEOL 2011 HRTEM, in order to determine the microstructural characteristics of the YSZ coating, as well as the resulted phases near the coating/substrate interface. Afterwards the as-coated samples were dipped in molten zinc at 450±5°C up to 144 hrs (6 days). At regular time intervals (every 24 hrs), coupons were withdrawn from the liquid phase and chemically treated with dilute aqueous solution of HCI to remove the residual molten metal. To quantify corrosion progress the weight loss of each coupon was determined. Uncoated St-37 coupons were also dipped in liquid zinc under the same conditions for comparison reasons. Furthermore for the study of the corrosion mechanism, cross-sections of the corroded samples were examined with SEM.

3. Results

3.1. Characterization of the coating structure

The examination of the coating reveals a very rough surface (Fig. 1). As it was calculated from micrographs similar to those of Fig. 2, the average values for R_a and R_{max} are respectively 17 and 29 μm. This phenomenon is not peculiar, if we take into account the deposition method used. This roughness results from the spreading, solidification and stacking of impinging particles. It depends on the feedstock particle sizes, their melting state (viscosity) and momentum at impact. Of course, unmolten or resolidified particles can locally modify the roughness, because part of the powder is totally or partially solidified before reaching the ferrous substrate or the already formed coating, since the freezing time of the flying droplets is very low [11]. Consequently entire solid spheres are trapped inside the deposited YSZ, as it is possible to be observed in the SEM micrograph of Fig. 1b. Moreover, the substrate roughness also plays a role on the coating surface roughness. In any case all these factors render impossible the formation of an even surface.

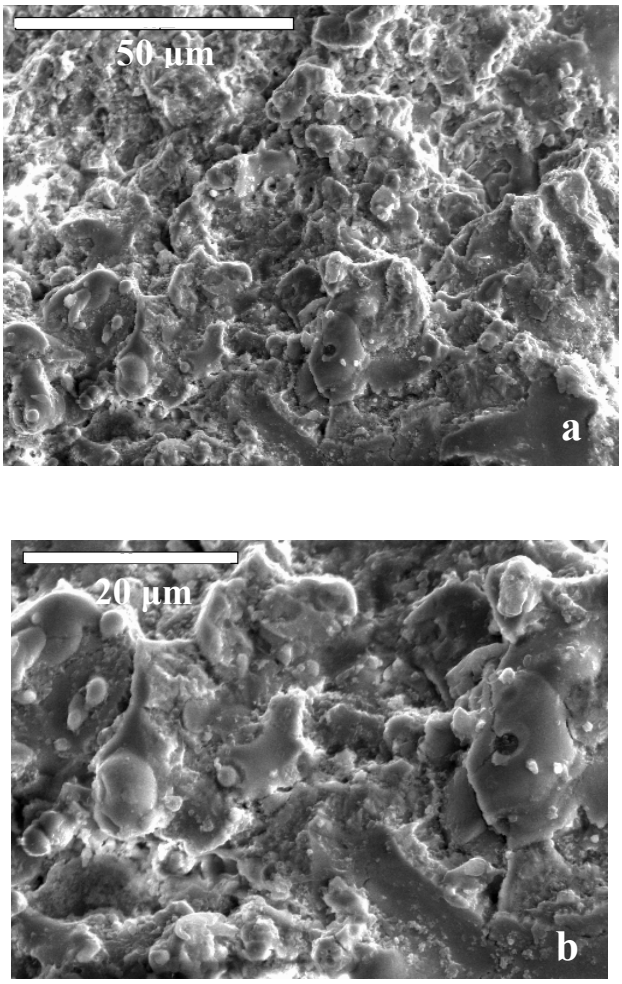

Fig. 1. SEM micrographs of the coating surface (a: at low magnification, b: at higher magnification).

The observation of the coating cross-section (Fig. 2) reveals also a highly inhomogeneous material. Pores and voids of different sizes and shapes are predominant. They are randomly scattered in the coating starting from the surface of the ferrous substrate up to the coating surface. However there are no areas where these pores are gathered but they are more or less uniformly distributed in the coating mass. Implementing image analysis, it is possible to calculate the ratio of the surface of their cross-section to the total surface of the cross-section of the coating. From this procedure it was deduced that they refer to about 15% of the coating volume. However they do not communicate with each other. As a result they do not form a network and thus there are no paths in the coating that could facilitate corrosion of the ferrous substrate.

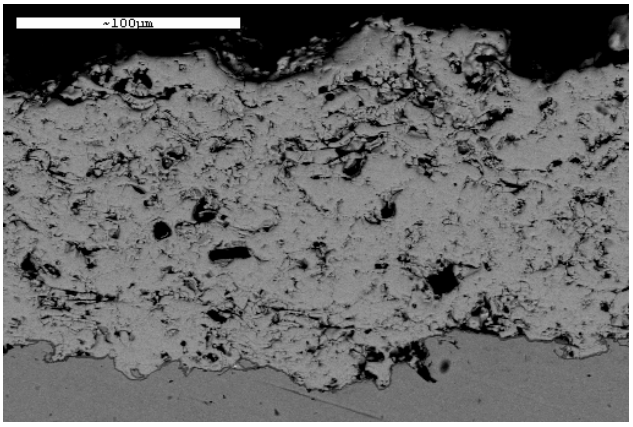

Fig. 2. SEM micrographs of the coating cross-section.

In any case the pore formation is an inherent disadvantage of the thermal sprayed coatings [12-13], because, as it was mentioned earlier, during thermal spraying the droplets that deposit at the substrate could be semi-molten or even solid and they collide with a more or less solid surface. As a result it is likely that they do not exactly fit the already formed pattern and hence cavities are formed around their contact points. Consequently as the molten fraction of the droplets decrease, the density of the cavities increases. This phenomenon is probably affected by differences in the deposition conditions, such as the gun-substrate distance, which could change the physical condition of the droplets However these phenomena were not investigated in this work.

EDS stoichiometric analysis of the coating cross-section showed that the coating is composed, as it was expected, only by yttrium, zirconium and oxygen. The composition of certain areas (Table I) is very close to the theoretical results drawn by the stoichiometry of the powder used for the coating deposition (ZrO_2- 8 mol% Y_2O_3). However in other areas different composition is observed referring to different yttria content ranging from 10 to 4 mol%. Consequently, the coating is not only morphological inhomogeneous, but it is also inhomogeneous from the compositional point of view. However no impurities or other elements were detected inside the coating. This observation is very important as far as it concerns the corrosion performance, since it implies that there are no inclusions in the coating that could trigger or facilitate corrosion.

Table 1. Average composition of the coating.

Element	Exp. Content (wt.%)	Theor. Content (wt.%)
Zr	60.2	63.85
Y	9.2	10.82
O	30.6	25.33

The EDS examination of the coating / substrate interface showed that no iron is present in the coating mass, while the oxides did not penetrate into the substrate lattice. Hence at the coating / substrate interface no diffusion takes place. Consequently the coating adhesion to the underlying phase is only mechanical and not metallurgical or chemical. For that purpose a rough substrate surface is required prior to coating deposition [6]. As a result the bond strength is expected to be comparatively low. If we take also into account the inherent brittleness of ceramics, it is obvious that YSZ coatings are very sensitive to mechanical damages. In the case of hot-dip galvanizing kettles this characteristic could be considered as a serious disadvantage of the coating, because the objects to be galvanized often come in contact with the kettle walls. As a result scratches could be caused especially at the sidewalls of the kettle, which expose the underlying steel facilitating its corrosion.

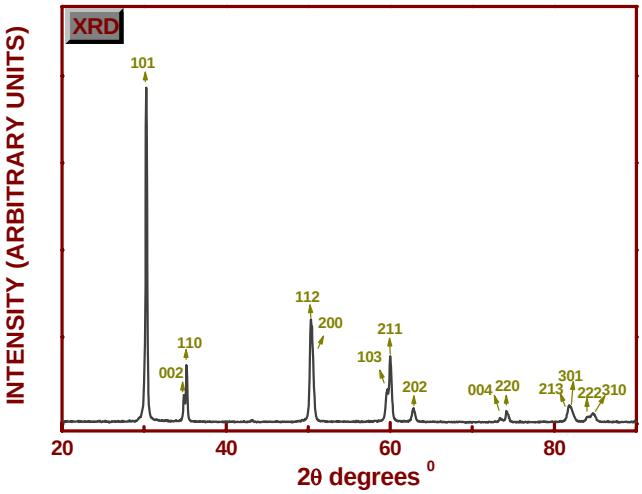

Fig. 3. XRD pattern of the YSZ coating referring to ZrO_2- 4.3 mol% Y_2O_3 (PDF# 82-1242) [14].

The coating structure was initially examined with XRD. The XRD pattern of Fig. 3 refers to YSZ with different stoichiometry than the theoretical (ZrO_2- 4.3 mol% Y_2O_3). In any case the XRD analysis is more representative with regard to the EDS since it averages the results of a much larger area. As a result it could be considered that the average composition of the coating is much closer to the XRD results. The recorded XRD pattern is very clear and consequently the crystal size is expected to be large. This observation is also beneficial for the corrosion performance of the coating because the existence of shorter grain boundaries impedes the coating degradation.

The coating structure was also examined with TEM. The TEM examination verified also the above results. Large crystals with a size of a few μm were detected (Fig. 4). The unit cell of these crystals was verified by comparing the calculated d_{hkl}-values with the

experimental ones measured from diffraction. The results of all these calculations are presented in Table 2.

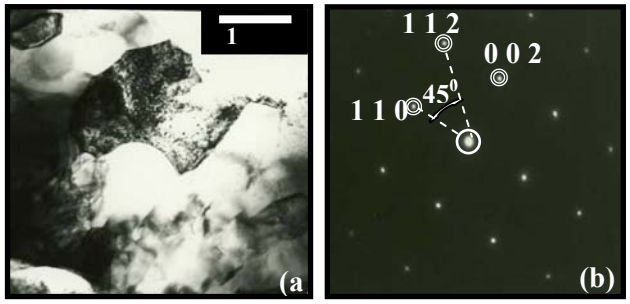

Fig. 4. Bright field TEM micrograph (a) and ED pattern (b) of the coating indicating a large crystal of ZrO_2:9,5%Y_2O_3 (PDF#82-1242) [14]. The hkl indices were identified in Table 2.

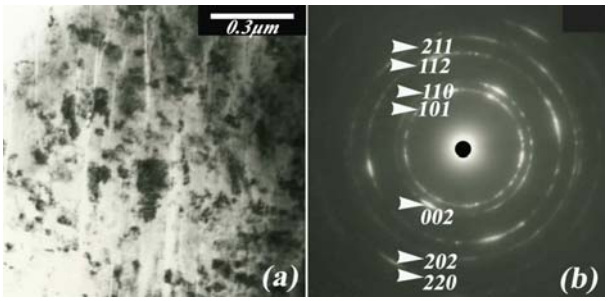

Fig. 5. *Bright field TEM micrograph (a) and ED pattern (b) of the coating indicating small crystals of ZrO_2:9,5%Y_2O_3 (PDF#82-1242) [14].*

Table 2. Experimental and calculated d-values for the indexed spots of the electron diffraction (ED) pattern of Fig. 4b.

hkl	d_{exp} (Å)	d_{cal} (Å)
112	1.81	1.818
110	2.57	2.562
002	2.58	2.579

Table 3. Experimental and calculated d-values for the indexed rings of the electron diffraction pattern of Fig. 5b (d-values in grey shade are denoted in the ED pattern).

hkl	d_{exp} (Å)	d_{cal} (Å)
101	2.97	2.965
002	2.58	2.579
110	2.57	2.562
112	1.83	1.818
200	1.82	1.812
103	1.56	1.553
211	1.55	1.546
004	1.29	1.289
220	1.28	1.281
202	1.48	1.482

However the larger resolution of TEM allowed us also to observe smaller crystals with dimensions of a few hundreds of nm (Fig. 5 and Table III) up to nanograins with average size less than 10 nm (Fig. 6), although the small size crystals refer only to a small fraction of the coating as the clarity of the XRD pattern implies. Furthermore different stoichiometries were recorded. Nevertheless, apart from Zr, Y and O, no other element was detected, although the examination was very detailed.

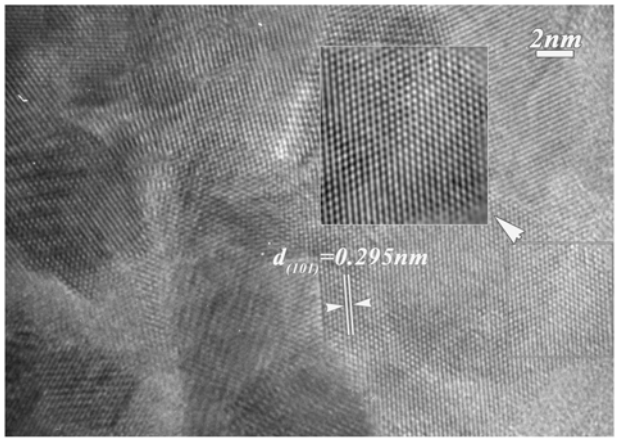

Fig. 6. HRTEM image of a nanocrystalline area. The lattice planes of the crystalline system $Y_xZr_yO_z$ are indicated. The reconstruction of an area in the tetragonal frame after the inverse Fourier Transformation is presented as an inset figure (PDF#82-1242) [14].

To sum up from, from the above examination it was deduced that the YSZ coatings are morphologically and compositionally inhomogeneous. More specifically, they are characterized by a large density of voids scattered in their mass, which however do not communicate with each other and thus they do not contribute to corrosion. Furthermore there is a large grain size distribution, starting from a few μm up to a few nm. However the larger part of the coating is composed by large size crystals which are advantageous as far as it concerns the corrosion performance. Nevertheless the different stoichiometries which were recorded refer only to Zr, Y and O. No other elements were detected which could act as nuclei facilitating corrosion. Consequently a good corrosion resistance is expected.

3.2 Corrosion performance

As it was mentioned before, it is likely the corrosion performance of YSZ coatings to be good. However it is not possible to have accurate results if corrosion experiments do not take place. For that purpose coupons of pure steel St-37 along with coated coupons were placed inside molten zinc under the same conditions (450±5°C). A typical photograph of an uncoated sample after 144 hrs of exposure in the liquid metal is presented in Fig. 7. This image is focused on the part of the coupon which was close at the surface of the liquid phase. The results of

corrosion are obvious. The splitting line between the submerged part of the coupon and the part which was outside the liquid is not even due to the fact that liquid zinc wets steel and as a result a positive meniscus is formed at their interface. Iron solubility in liquid zinc at this temperature is low [15], and as a result direct dissolution in this case is rather limited. However zinc reacts with iron forming several alloying compounds [15], which are insoluble in liquid zinc and precipitate in the crucible. Consequently Fe atoms are constantly transferred from the substrate to the liquid phase. Saturation does not occur because these atoms are withdrawn from the system through the formation of insoluble Fe-Zn crystals. Nevertheless corrosion is delayed because the Fe-Zn phases are also deposited on the surface of the ferrous substrate and thus a more corrosion resistant layer is formed on top of it. However corrosion is not totally inhibited, because Fe is diffused through this layer to the liquid phase. In any case the corrosion of the substrate seems to be uniform. Its kinetics is presented in the diagram of Fig. 8. From this diagram it possible to be deduced that the weight loss per surface unit is almost linear. However at high exposure (dipping) time a decline from the linear behaviour is recorded, which is probably due to the increase of the protective layer thickness.

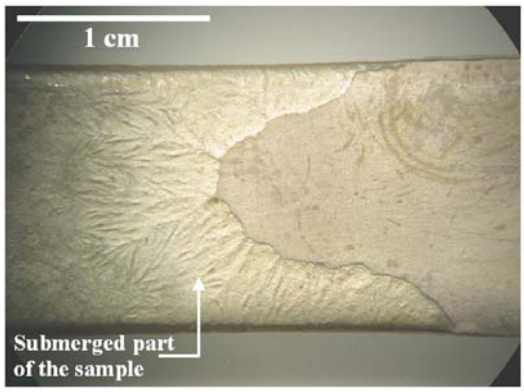

Fig. 7. Stereoscopic photograph of uncoated steel after 144 hrs of exposure in liquid zinc.

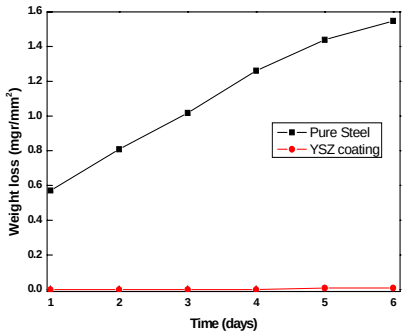

Fig. 8. Diagram of the weight loss per surface unit with regard toosure ping) time for the uncoated andasamples.

The performance of the YSZ coating under the same circumstances is outstanding, as the plot of Fig. 8 shows. The weight loss is almost zero, while zinc does not wet the coating. Hence YSZ offers excellent protection to the underlying steel.

4. Conclusions

From the above investigation it was turned out that the coating contains pores at large density, which do not affect its anticorrosive performance. Furthermore, the chemical composition varies from ZrO_2-10%Y_2O_3 to ZrO_2-4%Y_2O_3. However there are neither inclusions nor impurities, while the crystal size ranges from a few μm up to a few nm (nanocrystals). In any case most of the crystals are large. Regarding corrosion, resistance is excellent. YSZ coating is almost unaffected by the molten zinc.

References

[1] P. Maass, P. Peissker, Handbuch Feuerverzinken, Wiley-VCH, (1993).
[2] P. F. Tortoreli, Fundamentals of high temperature corrosion in liquid metals, pp. 56-60, Vol. 13-Corrosion, ASM, New York, 2000.
[3] D. N. Tsipas, G. K. Triantafyllidis, J. Kipkemoi Kiplagat, P. Psillaki, Mat. Lett. **37**, 128(1998) .
[4] S. Ahmaniemi, P. Vuoristo, T. Mantyla, C. Gualco, A. Bonadei, R. Di Maggio, Surf. Coat. Techn. **190**, 378 (2005).
[5] A. G. Evans, D.R. Mumm, J.W. Hutchinson, G.H. Meier, F.S. Pettit, Prog. Mat. Sci. **46**, 505 (2001).
[6] T.E. Strangman, Thin Solid Films, **127**, 93(1985).
[7] K. W. Schlichting, N. P. Padture, E. H. Jordan, M. Gell, Mat. Sci. Eng. A **342**, 120 (2003).
[9] U. Schulz, M. Schmücker, Mat. Sci. Eng. A, **276**, 1 (2000).
[10] V. Lughiw, D. R. Clarke, J. Am. Ceram. Soc. **88**, 2552 (2005).
[11] Y. Chen, G. Wang, H. Zhang, Thin Solid Films **390**, 13(2001).
[12] R.H. Unger, Vol. 13: Thermal Spray Coatings, in ASM Handbook, New York, 1996.
[13] H. Herman, S. Sampath, R. McCune, Mat. Bull., 17(2000).
[14] P. C. Powder Diffraction Files, Version 2.02, JCPDS-ICDD, 2000.
[15] A. R. Marder, Prog. Mat. Sci. **45**, 191(2000).

*Coressponding author: gvourlia@auth.gr